PIK3CA C-terminal frameshift mutations are novel oncogenic events that sensitize tumors to PI3K-α inhibition

Jennifer M. Spangle[a,1,2], Thanh Von[a,b], Dean C. Pavlick[c], Arina Khotimsky[b], Jean J. Zhao[a,b], and Thomas M. Roberts[a,b,2]

[a]Department of Biological Chemistry and Molecular Pharmacology, Harvard Medical School, Boston, MA 02115; [b]Department of Cancer Biology, Dana-Farber Cancer Institute, Boston, MA 02115; and [c]Foundation Medicine, Cambridge, MA 02141

Edited by Rene Bernards, The Netherlands Cancer Institute, Amsterdam, Netherlands, and approved August 5, 2020 (received for review January 2, 2020)

***PIK3CA* hotspot mutation is well established as an oncogenic driver event in cancer and its durable and efficacious inhibition is a focus in the development and testing of clinical cancer therapeutics. However, hundreds of cancer-associated *PIK3CA* mutations remain uncharacterized, their sensitivity to PI3K inhibitors unknown. Here, we describe a series of *PIK3CA* C-terminal mutations, primarily nucleotide insertions, that produce a frame-shifted protein product with an extended C terminus. We report that these mutations occur at a low frequency across multiple cancer subtypes, including breast, and are sufficient to drive oncogenic transformation in vitro and in vivo. We demonstrate that the oncogenicity of these mutant p110α proteins is dependent on p85 but not Ras association. P110α-selective pharmacologic inhibition blocks transformation in cells and mammary tumors characterized by *PIK3CA* C-terminal mutation. Taken together, these results suggest patients with breast and other tumors characterized by *PIK3CA* C-terminal frameshift mutations may derive benefit from p110α-selective inhibitors, including the recently FDA-approved alpelisib.**

PI3K | cancer | signal transduction

The phosphatidylinositol 3-kinase gene *PIK3CA* encodes the p110α catalytic isoform of PI3K and is one of the most frequently mutated genes across cancer subtypes, including 40% of breast cancers (1). While the Catalogue of Somatic Mutations in Cancer (COSMIC) and other sources indicate more than 3,000 somatic DNA aberrations in *PIK3CA* have been identified in breast cancer, more than 98% of breast cancer-associated *PIK3CA* mutations occur in two hotspots (2, 3). Located in the helical and kinase domains, E542K/E545K and H1047R mutations, respectively, produce hyperactivated p110α lipid kinases that activate PI3K effector signaling, thereby enhancing cellular proliferation, transformation, and survival (4, 5).

Association of p110α with receptor tyrosine kinases (RTKs) at the plasma membrane drives PI3K-mediated signal transduction. In the absence of activating signals such as growth factors or chemokines, the N-SH2 domain of regulatory PI3K subunit p85 binds to the helical domain of p110α, and in so doing, inhibits p110α (6). Positive stimuli initiate p85-mediated recruitment of p110α to active RTKs, and upon RTK binding, p110α inhibition by p85 is relieved. Previous research demonstrates that the $PIK3CA^{H1047R}$ protein product is dependent on p85 association for its oncogenic activity (7). In contrast, the helical domain $PIK3CA^{E542K/E545K}$ mutations retain oncogenic signaling in the absence of p85 association and instead are dependent on Ras-GTP binding for oncogenic transformation (8). Moreover, $PIK3CA^{H1047R}$ mutation induces localized structural changes which enhance the accessibility of the C-terminal tail of p110α. It has been shown that increasing the positive charge of the p110α C terminus via $PIK3CA^{H1047R}$ mutation enhances its association with the cellular membrane and lipid kinase activity, which contribute to its oncogenicity (9, 10).

The frequency of PI3K pathway activation across cancers, in part driven by oncogenic *PIK3CA* hotspot mutation, has fueled the development and testing of PI3K inhibitors. Originally developed as pan-PI3K inhibitors designed to inhibit all class I PI3K isoforms, recent efforts have largely shifted toward the development and testing of isoform-selective inhibitors that target a single PI3K isoform such as p110α, p110β, or p110δ (11, 12). Preclinical and clinical research also indicates that tumors characterized by p110α hotspot mutations such as H1047R are sensitive to PI3K inhibition, and as such, inhibitors designed to selectively inhibit hotspot-mutated p110α are also in clinical development. Recent FDA approval of the p110α-selective inhibitor alpelisib, to be used in combination with fulvestrant for the treatment of *PIK3CA*-mutated, hormone receptor positive, *HER2*-negative, advanced or metastatic breast cancer, highlights the clinical utility of this class of therapeutic agents (13). With the development and approval of these highly selective therapeutic agents, identifying patients whose PI3K-activated tumors will respond to alpelisib and other highly selective PI3K inhibitors is a task of critical importance.

Here we identify a series of C-terminal mutations, primarily single nucleotide insertions that occur in the final coding amino acid or the stop codon of *PIK3CA*, in breast and other cancers. We demonstrate that these mutations transform in vitro and in vivo and define p85 interaction as required for their oncogenicity.

Significance

While *PIK3CA* hotspot mutations frequently occur in solid cancers and in some contexts are therapeutically actionable, numerous other *PIK3CA* genomic alterations have been observed but remain uncharacterized. The authors identify C-terminal *PIK3CA* frameshift mutations as oncogenic driver events dependent on p85 binding in breast cancer and other cancers. Breast cell lines and tumors expressing *PIK3CA* frameshift mutations are sensitive to PI3K inhibition via alpelisib treatment. Patients with tumors characterized by these mutations may derive clinical benefit from p110α-selective inhibition.

Author contributions: J.M.S. and T.M.R. designed research; J.M.S., T.V., D.C.P., and A.K. performed research; J.M.S., D.C.P., and J.J.Z. contributed new reagents/analytic tools; J.M.S. analyzed data; and J.M.S. and T.M.R. wrote the paper.

Competing interest statement: T.M.R. has a consulting relationship with Novartis and iKang, is a founder of Crimson Biotech and Geode Therapeutics, and is a member of the corporate boards of Crimson Biotech and Geode Therapeutics. J.J.Z. is a founder and board director of Crimson Biotech and Geode Therapeutics. D.C.P. is an employee of Foundation Medicine and has equity interest in F. Hoffman-La Roche AG.

This article is a PNAS Direct Submission.

Published under the PNAS license.

[1]Present address: Department of Radiation Oncology, Winship Cancer Institute of Emory University, Atlanta, GA 30322.

[2]To whom correspondence may be addressed. Email: jennifer.spangle@emory.edu or thomas_roberts@dfci.harvard.edu.

This article contains supporting information online at https://www.pnas.org/lookup/suppl/doi:10.1073/pnas.2000060117/-/DCSupplemental.

First published September 14, 2020.

Tumors characterized by C-terminal *PIK3CA* mutation are sensitive to p110α-selective inhibition, suggesting that patients with tumors characterized by these mutations may respond to p110α inhibition. Lastly, next-generation sequencing of patient tumors identifies co-occurring mutations that suggest rational cotherapeutic strategies for patients with tumors characterized by these *PIK3CA*-activating mutations.

Results and Discussion

Using publicly available datasets, we first observed nucleotide insertions or substitutions in the final *PIK3CA* amino acid codon 1068 or the stop codon (1069), one of which was previously identified (3, 14). These insertions or substitutions are predicted to produce a frameshifted protein product extending the p110α C terminus three to four amino acids (Fig. 1*A*). In all cases, nucleotide insertion or substitution heavily biased the resulting amino acids to the positively charged residues arginine and/or lysine.

To determine whether nucleotide insertion and the resulting frameshift mutations at the *PIK3CA* C terminus function as oncogenic events, a panel of *PIK3CA* C-terminal mutations (PIK3CA-Ct) were overexpressed in p110α$^{f/f}$; p110β$^{f/f}$ mouse embryonic fibroblasts (MEFs). Endogenous p110α and p110β were then excised via Adeno-Cre infection to yield p110α$^{-/-}$; p110β$^{-/-}$ knockout MEFs (15). *PIK3CA*-Ct expression increases PI3K effector activation more efficiently than expression of wild-type p110α, similar to the characterized hotspot *PIK3CA*^{H1047R} oncogenic mutation, as indicated by AKT and S6 phosphorylation (Fig. 1*B*). Similar results were obtained in Rat1 cells stably expressing *PIK3CA*-Ct mutations (*SI Appendix*, Fig. S1*A*). Expression of *PIK3CA*-Ct is also sufficient to increase MEF cell proliferation and the ability of MEFs to form foci comparable to *PIK3CA*^{H1047R} (Fig. 1 *C* and *D* and *SI Appendix*, Fig. S1*B*).

To address whether *PIK3CA*-Ct expression transforms in vitro and in vivo, we utilized hTERT immortalized human mammary epithelial cells (HMECs) that express a dominant negative p53 mutant (DD). These HMEC-DD cells are untransformed and cannot participate in anchorage independent growth. The expression of neuT (nT), an activated form of the Her2/neu oncogene, weakly transforms HMEC-DD cells. The addition of *PIK3CA* oncogenic alleles such as PIK3CA^{H1047R} strongly transforms HMEC-DDnT cells (16). We engineered HMEC-DDnT cells to express the panel of *PIK3CA*-Ct mutations (*SI Appendix*, Fig. S1*C*) to use in in vitro and in vivo oncogenesis assays. *PIK3CA*-Ct

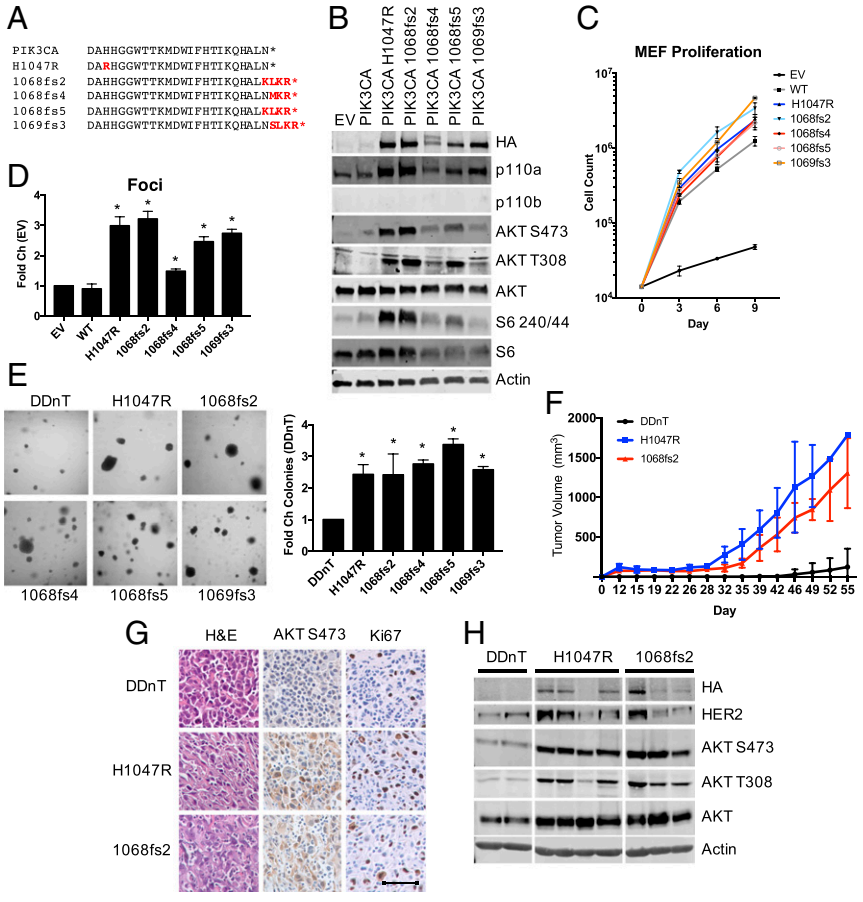

Fig. 1. *PIK3CA* C-terminal mutation is associated with human cancer, activates PI3K effector signaling, and transforms in vitro and in vivo. (*A*) Comparison of the C-terminal amino acid sequence of wild-type *PIK3CA* with cancer-associated *PIK3CA* genomic alterations (red). (*B*) HA-*PIK3CA* mutant overexpressing p110α$^{-/-}$; p110β$^{-/-}$ MEFs were starved for 4 h and subjected to immunoblotting with the indicated antibodies. (*C*) Cell proliferation was measured in HA-*PIK3CA* mutant overexpressing p110α$^{-/-}$; p110β$^{-/-}$ MEFs. Cells were reseeded and counted every 3 d to establish cell proliferation rates; $n = 3$. (*D*) Quantification of crystal violet staining of HA-*PIK3CA* mutant overexpressing p110α$^{-/-}$; p110β$^{-/-}$ MEFs. $^*P < 0.05$; unpaired *t* test; $n = 2$. (*E*) Images of cell suspensions of the indicated HA-*PIK3CA* mutant expressing HMECs were grown in soft agar (*Right*) and quantified (*Left*); $n = 3$. (*F*) Tumor volume of HMEC-DDnT cells of the indicated genotype injected into the mammary fat pads of nude mice. End point tumor volumes: DDnT, 122.5 ± 231.9 mm^3; DDnT HA-*PIK3CA*^{H1047R}, 1783.6 ± 0.0 mm^3; and DDnT HA-*PIK3CA*^{1068fs2}, 1304.7 ± 441.8 mm^3. Means ± SEM are shown; all groups $n \geq 8$; two-way ANOVA with Tukey's multiple-comparisons test. (*G*) Tumors derived from mice in *F*. Sections are stained with the indicated antibodies, randomly selected images shown. (Scale bar, 50 μM.) $n = 3$ mice/condition. (*H*) Lysates prepared from tumors isolated from mice in *F*. Lysates were immunoblotted with the indicated antibodies.

expression is sufficient to enable efficient growth of HMEC-DDnT cells in soft agar (Fig. 1*E*). Because *PIK3CA*^{1068fs2} expression robustly activates PI3K effector signaling and promotes transformation in in vitro assays, HMEC-DDnT cells expressing this mutation were selected for in vivo xenografts. Expression of *PIK3CA*^{1068fs2} results in tumor growth in nude mice comparable to *PIK3CA*^{H1047R} (Fig. 1*F* and *SI Appendix*, Fig. S1*D*). Tumors derived from HMEC-DDnT; *PIK3CA*^{1068fs2} mice are characterized by elevated PI3K effector signaling (Fig. 1 *G* and *H*).

Oncogenic *PIK3CA* mutations have been shown to drive oncogenicity through several distinct mechanisms. *PIK3CA*$^{E542K/E545K}$ helical domain mutations produce a mutant p110α that is dependent on Ras binding to signal to downstream effectors (7). Loss of Ras binding through *PIK3CA* K227E mutation reduces *PIK3CA*$^{E542K/E545K}$-mediated effector phosphorylation and abrogates its ability to transform. In contrast, the oncogenicity of *PIK3CA* catalytic domain mutations such as *PIK3CA*^{H1047R} is dependent on p85 association. Loss of p85 binding blocks *PIK3CA*^{H1047R}-mediated effector phosphorylation and transformation (7, 17). To understand the mechanism by which *PIK3CA*-Ct is oncogenic, HMEC-DDnT *PIK3CA*^{1068fs2} cells, in which the *PIK3CA*^{1068fs2} allele contains an additional mutation either abolishing p110α Ras binding (K227E) or p85 association (PBD), were utilized in transformation assays. The results of these assays demonstrate that *PIK3CA*^{1068fs2} is dependent on p85 binding, but not RAS binding, to increase effector phosphorylation (Fig. 2 *A* and *B* and *SI Appendix*, Fig. S2*A*) and enhance anchorage independent growth (Fig. 2 *C* and *D*), similar to *PIK3CA*^{H1047R}.

In recent years, PI3K-targeted therapies, namely isoform-selective PI3K inhibitors, have progressed in phase I to III clinical trials, and several are now FDA approved for specific

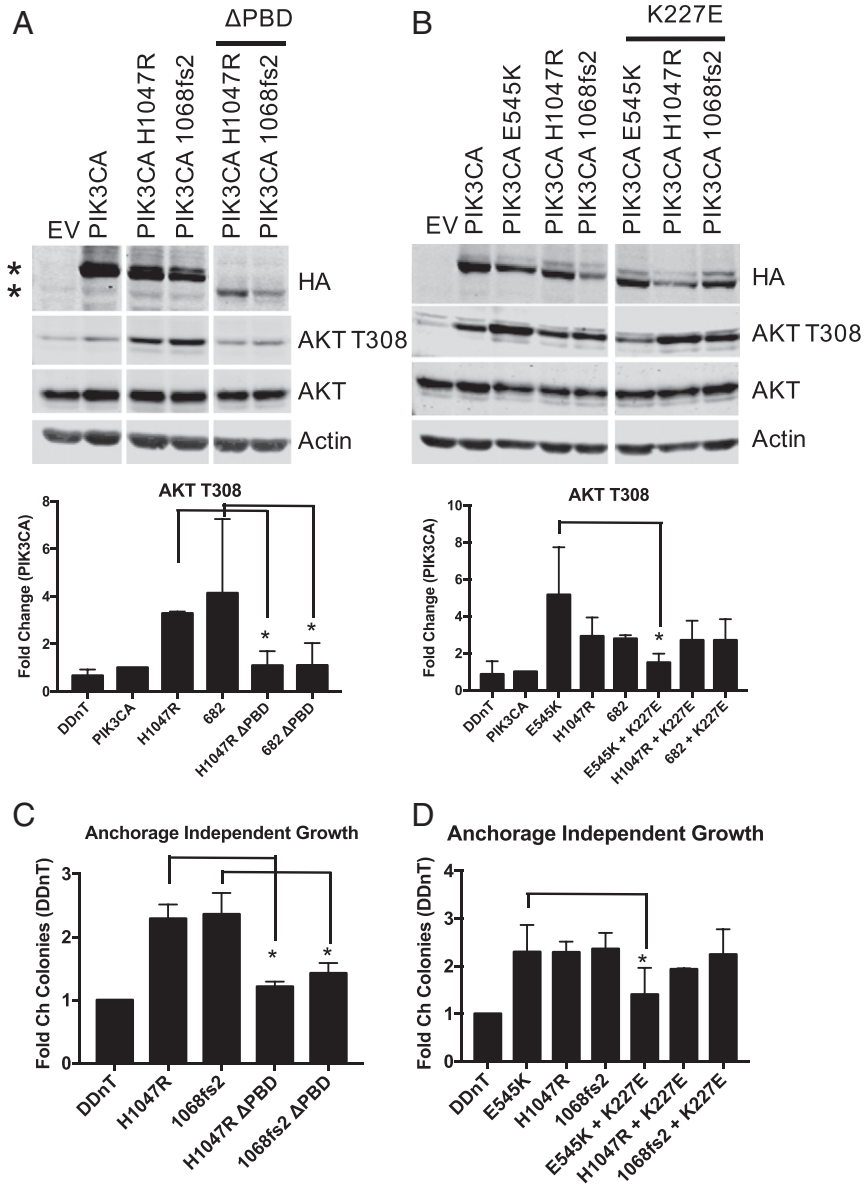

Fig. 2. *PIK3CA* C-terminal oncogenic transformation is dependent on p85 binding. HMEC-DDnT HA-*PIK3CA* mutant cells in which *PIK3CA* mutants possess abrogated p85 binding (*A*) or loss of Ras binding (*B*) were starved for 4 h and subjected to immunoblotting with the indicated antibodies (*Top*); * indicates p110α variant. Quantification of phospho-AKTT308 is shown (*Bottom*). (*C* and *D*) HMEC-DDnT HA-*PIK3CA* double mutant cells described in *A* and *B* were grown in soft agar and quantified; $n = 2$. Means ± SEM are shown; $^*P < 0.05$; unpaired *t* test.

indications, including alpelisib, idelalisib, and copanlisib (1, 13). However, a limitation in optimizing the clinical utility of these inhibitors is insufficient knowledge of the genomic and proteomic background which modulates sensitivity and resistance to these agents. To determine whether cell lines and tumors characterized by *PIK3CA*-Ct are sensitive to PI3K inhibition, cells that overexpress *PIK3CA*-Ct were treated with the pan-PI3K inhibitor pictilisib (pic), the p110α-selective inhibitor alpelisib (alp), or the p110β-selective inhibitor AZD6482 (AZD). PI3K effector phosphorylation is reduced in *PIK3CA*-Ct expressing p110α$^{-/-}$; p110β$^{-/-}$ knockout MEFs when treated with pan-PI3K or p110α-selective inhibitors, but as expected, not the p110β-selective inhibitor AZD6482 (Fig. 3*A*); similar results were obtained in HMECs (*SI Appendix*, Fig. S3*A*). Moreover, the ability of these cells to form foci is abrogated following either pan-PI3K or p110α-selective inhibition (Fig. 3*B* and *SI Appendix*, Fig. S3*B*). To address whether tumors characterized by *PIK3CA*-Ct are sensitive to PI3K inhibition, HMEC-DDnT *PIK3CA*^{H1047R} and HMEC-DDnT *PIK3CA*^{1068fs2} cells were transplanted into nude mice. Palpable tumors were treated with vehicle or alpelisib. HMEC-DDnT *PIK3CA*^{1068fs2} tumors were sensitive to p110α-selective inhibition (Fig. 3*C* and *SI Appendix*, Fig. S3*C*). Alpelisib-treated HMEC-DDnT *PIK3CA*^{1068fs2} tumors are significantly smaller (Fig. 3*D*) and are characterized by reduced AKT and S6 phosphorylation (Fig. 3 *E* and *F*). Taken together, our data suggest that tumors characterized by *PIK3CA*-Ct mutation are sensitive to p110α-selective inhibition and patients with tumors characterized by these mutations may be suitable candidates for clinical trials testing pan-or p110α-selective PI3K inhibitors.

The major limitations of clinical PI3K inhibition include identifying the patient population(s) which may benefit from PI3K-targeted therapy and preventing tumor recurrence or relapse. Next-generation sequence data derived from a comprehensive primary patient tumor dataset consisting of 233,272 unique patient tumors across solid tumor types were analyzed, and we identified 138 patient tumors characterized by 1 of 71 distinct genomic alterations that occur within the last four C-terminal *PIK3CA* amino acids or the stop codon (Dataset S1). While most detected alterations are nucleotide insertions, nucleotide deletions and substitutions were also observed. Of these distinct genomic alterations, 17 were identified in more than one patient tumor, with the highest frequency being N1068fs*5 (n = 47) (Fig. 4*A*). While *PIK3CA*-Ct alteration is frequently observed in breast cancer (n = 56), these genomic alterations were identified in other cancer types including uterine (n = 21), colon (n = 17), and lung cancers (n = 11) (Fig. 4*B*). These data suggest that tumors characterized by the oncogenic driver *PIK3CA*-Ct alterations can be detected using commercially available and validated cancer diagnostics at a low, but recurring, frequency in breast and other cancers. More than half of the breast tumors characterized by *PIK3CA*-Ct alteration lack other known PI3K pathway-activating genomic alterations (Fig. 4 *C* and *D* and Dataset S2), and genomic alterations in other key signaling pathways, proteins, or cellular processes including the CyclinD/Cdk4/6 axis, *ESR1*, *FGF*/*FGFR*, or *BRCA2* frequently occur (Fig. 4*D*). Of the breast tumors that contain additional PI3K pathway alterations, detected alterations include *PTEN* deletion or mutation, *PIK3CA* hotspot mutation, and amplification of AKT isoforms (*SI Appendix*, Fig. S4*A*). Other tumor types showed different propensity to harbor additional alterations in the PI3K pathway (*SI Appendix*, Fig. S4*B*). These data support our in vitro and in vivo findings that suggest *PIK3CA*-Ct genomic alterations are bona fide oncogenic driver events. Moreover, these data identify co-occurring, and in some cases, potentially actionable genomic alterations, in patients whose tumors are characterized by these mutations.

Collectively, our data support the notion that *PIK3CA*-Ct insertions are oncogenic. At this time, the transforming capacity of several nonhotspot *PIK3CA* mutations has been studied. Some missense mutations (e.g., N345K and C420R), while also infrequent, transform as efficiently as H1047R or E545K (18). Recently, the short indel *PIK3CA*$^{delP447\text{-}L455}$ was identified in a tumor from a patient with an advanced stage ER^{+}/endocrine therapy-resistant breast cancer (19). After receiving a combination of alpelisib and the aromatase inhibitor letrozole, the patient exhibited an 11-mo sustained clinical response, a finding which supports the hypothesis that other nonhotspot *PIK3CA* mutations, including indels, may be sensitive to PI3K-targeted therapies (19). Generally, indels are rare in oncogenes and more frequently occur in tumor suppressors such as *TP53* or *PTEN*, resulting in the functional inactivation of the protein product. However, computational modeling and in vitro experiments demonstrate that because the deleted residues occur in the *PIK3CA* C2 domain involved in p85 association, *PIK3CA*$^{delP447\text{-}L455}$ is oncogenic through the modulation of p85 binding (19). Our results also show that the oncogenicity of *PIK3CA*-Ct mutants is at least in part dependent on p85 binding (Fig. 2). Of note, the *PIK3CA*-Ct mutations observed here increase the Ct positive charge via the introduction of R/K residues, as does the H1047R hotspot mutation. We hypothesize that the oncogenicity of *PIK3CA*-Ct mutants is augmented by the increased local positive charge, which enhances association with the negatively charged inner leaflet of the plasma membrane, thereby increasing the lipid kinase output of the enzyme, similar to what has been reported for *PIK3CA*^{H1047R} (9, 20).

The identification and characterization of a class of *PIK3CA* mutations that are sensitive to the FDA-approved, p110α-selective inhibitor alpelisib is timely. In an effort to further increase the selectivity of PI3K inhibitors, many next-generation inhibitors are being designed to selectively target cancer-associated mutant p110α proteins such as *PIK3CA*^{H1047R}. We do not predict that tumors characterized by *PIK3CA*-Ct mutations would demonstrate enhanced sensitivity to inhibitors targeting these well-characterized *PIK3CA* mutations. However, these data suggest that an inhibitor designed to target p110 association with the plasma membrane may exhibit increased efficacy in tumors characterized by this unique class of *PIK3CA* mutations. Lastly, the data presented here suggest opportunities for the preclinical testing of combination therapies; CyclinD/*CDK4/6* or *BRCA2* alteration frequently co-occur in breast tumors characterized by *PIK3CA*-Ct mutations. Thus, it is appropriate to investigate whether patients with breast tumors characterized by these actionable genomic alterations may benefit from combination CDK4/6 or PARP inhibition with alpelisib, as has been evaluated for breast tumors characterized by hotspot *PIK3CA* mutation.

Materials and Methods

Cell Lines and Inhibitors. HA-*PIK3CA* overexpressing p110α$^{-/-}$; p110β$^{-/-}$ knockout MEFs were generated as previously described (15). HMEC-derived cell lines were maintained in Dulbecco's Modified Eagle Media (DMEM) /F12 supplemented with 0.01 μg/mL epidermal growth factor (EGF), 10 μg/mL insulin, 0.025 μg/mL hydrocortisone, 1 ng/mL cholera toxin, 0.6% fetal bovine serum (FBS), 1% penicillin-streptomycin (pen-strep) and MEFs maintained in DMEM + 10% FBS and 1% pen-strep, each at 37 °C and 5% CO_2. Pictilisib, alpelisib, and AZD6482 were purchased from Selleck.

Plasmids. *PIK3CA* C-terminal insertion mutants were generated using a two-step site-directed mutagenesis (Agilent) into the wild-type pBabe HA-*PIK3CA* vector (16). Site-directed mutagenesis was first used to introduce nucleotides from the endogenous *Homo sapiens PIK3CA* open reading frame (ORF) immediately downstream of the *PIK3CA* stop codon, to produce pBabe HA-*PIK3CA*+CT. Point mutations introducing the described nucleotide insertions that occur in the *PIK3CA* ORF were then generated in the pBabe

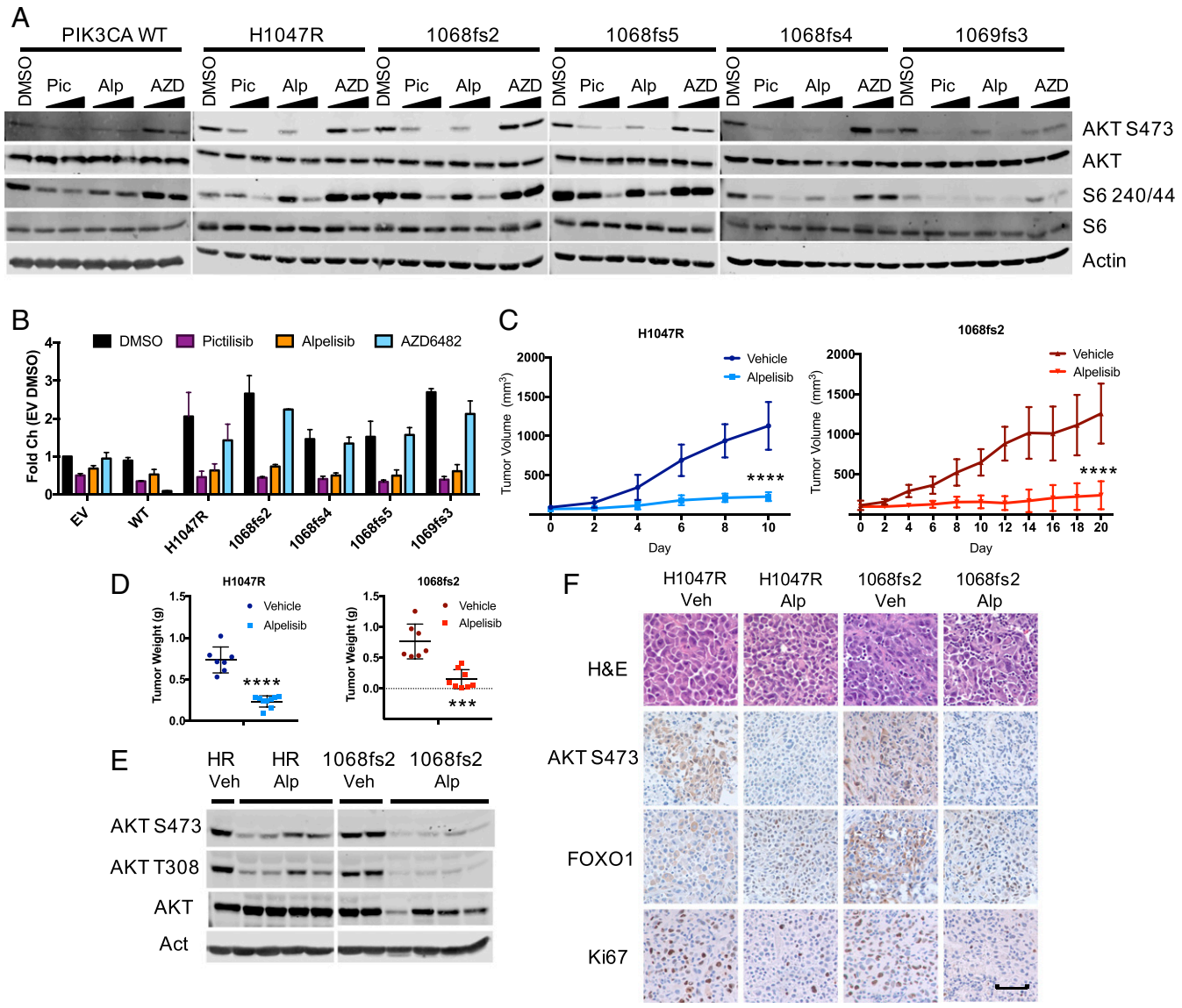

Fig. 3. Cell lines and tumors characterized by *PIK3CA* C-terminal mutation are sensitive to PI3K inhibition. (*A*) HA-*PIK3CA* variant overexpressing p110α$^{-/-}$; p110β$^{-/-}$ MEFs were starved for 4 h in the presence of pictilisib (1 μM), alpelisib (1 μM), or AZD6482 (1 μM) before immunoblotting with the indicated antibodies. (*B*) Crystal violet staining of HA-*PIK3CA* mutant overexpressing p110α$^{-/-}$; p110β$^{-/-}$ MEFs (*Left*) and quantification to measure foci formation by extracted stain (*Right*); $n = 2$. (*C*) Tumor volume of HMEC-DDnT *PIK3CA*^{H1047R} (*Left*) and HMEC-DDnT *PIK3CA*^{1068fs2} (*Right*) tumors orthotopically transplanted into the mammary fat pads of nude mice with once-daily treatment (45 mg/kg, gavage) with alpelisib. End point tumor volumes: DDnT HA-*PIK3CA*^{H1047R} Veh, 1128.2 ± 303.9 mm^3; DDnT HA-*PIK3CA*^{H1047R} alpelisib, 229.1 ± 56.1 mm^3; DDnT HA-*PIK3CA*^{1068fs2} Veh, 1259.5 ± 375.1 mm^3; and DDnT HA-*PIK3CA*^{1068fs2} alpelisib, 237.1 ± 175.1 mm^3. Means ± SEM are shown; all groups $n \geq 7$; two-way ANOVA with Tukey's multiple-comparisons test. ****$P < 0.0001$. (*D*) The wet weight of individual mammary tumors plus associated mammary gland tissue from *PIK3CA*^{H1047R} vehicle ($n = 7$), *PIK3CA*^{H1047R} alpelisib ($n = 9$) (*Left*), *PIK3CA*^{1068fs2} vehicle ($n = 7$), and *PIK3CA*^{1068fs2} alpelisib ($n = 8$) (*Right*). *PIK3CA*^{H1047R} and *PIK3CA*^{1068fs2} tumors were harvested 10 and 21 d from treatment onset, respectively. Means ± SEM are shown. ***$P < 0.001$; ****$P < 0.0001$; unpaired *t* test. (*E*) Lysates prepared from tumors isolated from mice in *C* and immunoblotted with the indicated antibodies. (*F*) Tumors derived from mice in *C*. Sections are stained with the indicated antibodies, randomly selected images shown. (Scale bar, 50 μM.) $n = 3$ mice/condition.

HA-*PIK3CA*+CT vector. Plasmids were sequence verified, packaged into retroviral particles, and used to generate stable MEF and HMEC cell lines.

Animal Xenograft Models and In Vivo Treatment Studies. A total of 4 × 10^6 HMEC cells were resuspended in 40% Matrigel (BD) and injected into the third mammary fat pads of athymic nude mice and palpable tumors were measured every 3 d. For the PI3K-inhibitor studies, tumors originating in donor mice were harvested and fragments implanted into the third mammary fat pads of recipient athymic nude mice. Where applicable, alpelisib was reconstituted in 0.5% methylcellulose (Sigma) and administered by oral gavage (45 mg/kg) once daily for at least 7 d prior to tumor isolation and preparation. Tumors were isolated and prepared within 3 h of treatment. All mouse experiments were conducted in accordance with protocols approved by the Institutional Animal Care and Use Committees of Dana-Farber Cancer Institute and Harvard Medical School (HMS).

Immunohistochemistry. Formalin-fixed, paraffin-embedded (FFPE) prepared tumors were sectioned (HMS Rodent Histopathology Core) and mounted. Immunohistochemical staining was performed using a sodium citrate antigen retrieval method (Boston BioProducts). Slides were blocked and incubated in primary antibody overnight (4 °C): AKTS473 (CST 4060), HER2 (Origene UM500036), pS6 (CST 5364), and Ki67 (Vector VP-RM04). Antibody signal was detected using biotinylated secondary antibody, 3,3-diaminobenzidine (DAB) developed (Vector Labs), and counterstained with hematoxylin (Vector Labs). Sections were mounted and imaged (Nikon Eclipse E600).

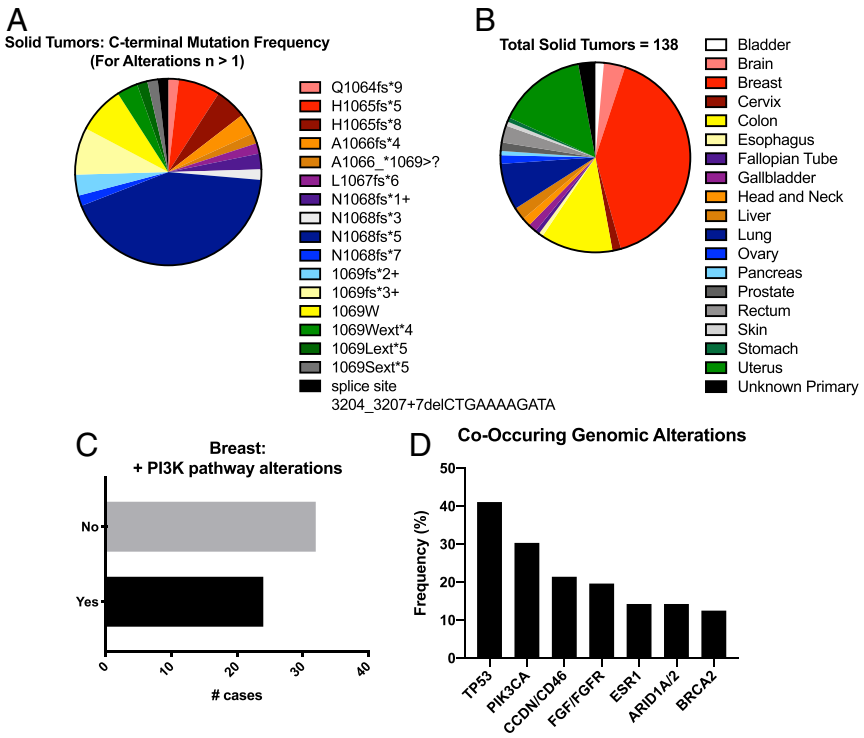

Fig. 4. *PIK3CA*-Ct mutations occur across human cancers and co-occur with actionable genomic alterations. (*A*) Identity and frequency of *PIK3CA*-Ct mutations in solid human tumors for alterations, $n > 1$. (*B*) Prevalence of *PIK3CA*-Ct mutations across tumor types. (*C*) Frequency of additional PI3K pathway alterations in breast cancer. (*D*) Co-occurring genomic alterations in breast cancer.

Cell/Tissue Lysis, Immunoblotting, and Immunoprecipitation. Cells were lysed in immunoprecipitation buffer (20 mM Tris HCl pH 7.5, 150 mM NaCl, 5 mM $MgCl_2$, 1% Nonidet P-40), supplemented with protease and phosphatase inhibitors. Tissue was homogenized by mixing with lysis buffer with beads and pulsing in a tissue homogenizer (BioRuptor). Cell and tissue lysates were separated using sodium dodecyl sulfate/polyacrylamide gel electrophoresis (SDS/PAGE). Proteins were transferred to nitrocellulose membranes and blocked in tris buffered saline containing tween-20 (TBST) + 5% milk and proteins of interest were visualized after primary and secondary antibody incubation (Odyssey, Li-Cor). Primary antibodies were as follows: AKT (9272), AKTT308 (13038), AKTS473 (9271), HA (2367), p110α (4249), p110β (3011), HER2 (4290), S6 (2217), S6S240/44 (2215) (CST), p85α (MABS831), and β-actin (MAB1501) (Millipore). For immunoprecipitations, lysates and antibodies were incubated and then conjugated to Protein A/G beads (Invitrogen). Beads were washed and associated proteins separated by SDS/PAGE.

Transformation Assays. For cell proliferation assays, 14,000 MEFs were initially seeded in 6-well dishes and counted every 3 d, at which time 14,000 cells were reseeded. At the end of the experiment, the total cell numbers were calculated. A total of 4,500 MEFs were seeded in 12-well dishes for focus formation assays and media changed every 3 d. After 2 wk, cells were fixed and crystal violet stained. Crystal violet was quantified by destaining in MeOH and measuring the OD590. Anchorage independent growth was measured by seeding 4,500 HMEC cells in 12-well plates in a solution of 0.3% agar in HMEC media on top of a base layer of 0.6% agar in DMEM. Images of unstained colonies were taken (Nikon) and plates were then stained with 0.5 mg/mL iodonitrotetrazolium chloride (Sigma) and images collected (Alpha Innotech).

Patient Data. Comprehensive genomic profiling (CGP) was performed on hybridization-captured, adaptor ligation-based libraries of $n = 219{,}861$ consecutive and research-consented solid-tumor patient specimens using the FoundationOne and FoundationOne CDx platforms, as previously described (21). All tumors characterized by genomic *PIK3CA* C-terminal frameshift insertions and deletions within or after amino acid Q1064 were deidentified and included in this dataset. The prevalence and identity of additional PI3K pathway alterations were also provided for the solid tumor cohort. The complete genomic profiles for breast tumors which met the above selection criteria were provided.

Data Availability. The authors confirm that the data supporting the findings of this study, along with protocols, are available within the article and/or its supplementary materials. Reagents and additional information are available upon request.

ACKNOWLEDGMENTS. We apologize to the colleagues whose impactful work we were unable to cite due to space limitations. We thank Drs. Heilmann, Bergholz-Villafane, and Ni for technical advice. This study was supported in part by grants from the NIH (K99 CA204601-01A1 to J.M.S.) and SU2C (SU2C-AACR-DT0209 to T.M.R. and J.J.Z.).

1. L. M. Thorpe, H. Yuzugullu, J. J. Zhao, PI3K in cancer: Divergent roles of isoforms, modes of activation and therapeutic targeting. *Nat. Rev. Cancer* **15**, 7–24 (2015).
2. T. Dogruluk *et al*., Identification of variant-specific functions of PIK3CA by rapid phenotyping of rare mutations. *Cancer Res.* **75**, 5341–5354 (2015).
3. Y. Zhang *et al*., A pan-cancer proteogenomic atlas of PI3K/AKT/mTOR pathway alterations. *Cancer Cell* **31**, 820–832.e3 (2017).
4. A. G. Bader, S. Kang, P. K. Vogt, Cancer-specific mutations in PIK3CA are oncogenic in vivo. *Proc. Natl. Acad. Sci. U.S.A.* **103**, 1475–1479 (2006).
5. J. J. Zhao *et al*., The oncogenic properties of mutant p110alpha and p110beta phosphatidylinositol 3-kinases in human mammary epithelial cells. *Proc. Natl. Acad. Sci. U.S.A.* **102**, 18443–18448 (2005).
6. C. H. Huang *et al*., The structure of a human p110alpha/p85alpha complex elucidates the effects of oncogenic PI3Kalpha mutations. *Science* **318**, 1744–1748 (2007).
7. L. Zhao, P. K. Vogt, Helical domain and kinase domain mutations in p110alpha of phosphatidylinositol 3-kinase induce gain of function by different mechanisms. *Proc. Natl. Acad. Sci. U.S.A.* **105**, 2652–2657 (2008).
8. N. Miled *et al*., Mechanism of two classes of cancer mutations in the phosphoinositide 3-kinase catalytic subunit. *Science* **317**, 239–242 (2007).
9. P. Gkeka *et al*., Investigating the structure and dynamics of the PIK3CA wild-type and H1047R oncogenic mutant. *PLoS Comput. Biol.* **10**, e1003895 (2014).
10. D. Mandelker *et al*., A frequent kinase domain mutation that changes the interaction between PI3Kalpha and the membrane. *Proc. Natl. Acad. Sci. U.S.A.* **106**, 16996–17001 (2009).
11. C. Fritsch *et al*., Characterization of the novel and specific PI3Kα inhibitor NVP-BYL719 and development of the patient stratification strategy for clinical trials. *Mol. Cancer Ther.* **13**, 1117–1129 (2014).

12. P. Liu *et al*., Oncogenic PIK3CA-driven mammary tumors frequently recur via PI3K pathway-dependent and PI3K pathway-independent mechanisms. *Nat. Med.* **17**, 1116–1120 (2011).
13. F. André *et al*.; SOLAR-1 Study Group, Alpelisib for *PIK3CA*-mutated, hormone receptor-positive advanced breast cancer. *N. Engl. J. Med.* **380**, 1929–1940 (2019).
14. J. G. Tate *et al*., COSMIC: The catalogue of somatic mutations in cancer. *Nucleic Acids Res.* **47**, D941–D947 (2019).
15. O. Cizmecioglu, J. Ni, S. Xie, J. J. Zhao, T. M. Roberts, Rac1-mediated membrane raft localization of PI3K/p110β is required for its activation by GPCRs or PTEN loss. *eLife* **5**, e17635 (2016).
16. J. J. Zhao *et al*., The p110alpha isoform of PI3K is essential for proper growth factor signaling and oncogenic transformation. *Proc. Natl. Acad. Sci. U.S.A.* **103**, 16296–16300 (2006).
17. L. Zhao, P. K. Vogt, Hot-spot mutations in p110alpha of phosphatidylinositol 3-kinase (pI3K): Differential interactions with the regulatory subunit p85 and with RAS. *Cell Cycle* **9**, 596–600 (2010).
18. M. Gymnopoulos, M. A. Elsliger, P. K. Vogt, Rare cancer-specific mutations in PIK3CA show gain of function. *Proc. Natl. Acad. Sci. U.S.A.* **104**, 5569–5574 (2007).
19. S. Croessmann *et al*., PIK3CA C2 domain deletions hyperactivate phosphoinositide 3-kinase (PI3K), generate oncogene dependence and are exquisitely sensitive to PI3Kalpha inhibitors. *Clin. Cancer Res.* **24**, 1426–1435 (2017).
20. Y. Samuels *et al*., High frequency of mutations of the PIK3CA gene in human cancers. *Science* **304**, 554 (2004).
21. G. M. Frampton *et al*., Development and validation of a clinical cancer genomic profiling test based on massively parallel DNA sequencing. *Nature Biotechnology*, 1023–1031, 10.1038/nbt.2696 (2013).